Cell

LSD1 Is a Subunit of the NuRD Complex and Targets the Metastasis Programs in Breast Cancer

Yan Wang,[1] Hua Zhang,[1] Yupeng Chen,[1] Yimin Sun,[1] Fen Yang,[1] Wenhua Yu,[1] Jing Liang,[1] Luyang Sun,[1] Xiaohan Yang,[1] Lei Shi,[1] Ruifang Li,[1] Yanyan Li,[1] Yu Zhang,[1] Qian Li,[1] Xia Yi,[1] and Yongfeng Shang[1,*]

[1]Key Laboratory of Carcinogenesis and Translational Research, Ministry of Education, Department of Biochemistry and Molecular Biology, Peking University Health Science Center, Beijing 100191, China

*Correspondence: yshang@hsc.pku.edu.cn

DOI 10.1016/j.cell.2009.05.050

SUMMARY

Lysine-specific demethylase 1 (LSD1) exerts pathway-specific activity in animal development and has been linked to several high-risk cancers. Here, we report that LSD1 is an integral component of the Mi-2/nucleosome remodeling and deacetylase (NuRD) complex. Transcriptional target analysis revealed that the LSD1/NuRD complexes regulate several cellular signaling pathways including TGFβ1 signaling pathway that are critically involved in cell proliferation, survival, and epithelial-to-mesenchymal transition. We demonstrated that LSD1 inhibits the invasion of breast cancer cells in vitro and suppresses breast cancer metastatic potential in vivo. We found that LSD1 is downregulated in breast carcinomas and that its level of expression is negatively correlated with that of TGFβ1. Our data provide a molecular basis for the interplay of histone demethylation and deacetylation in chromatin remodeling. By enlisting LSD1, the NuRD complex expands its chromatin remodeling capacity to include ATPase, histone deacetylase, and histone demethylase.

INTRODUCTION

Lysine specific demethylase 1 (LSD1/BHC110/KIAA0601/p110b/AOF2/KDM1) is an amine oxidase that catalyzes histone demethylation via a flavin adenine dinucleotide (FAD)-dependent oxidative reaction (Lan et al., 2008; Shi et al., 2004). Biochemically, LSD1 acts to remove the mono- and di-methyl moieties from H3-K4 and, functionally, LSD1 impacts on the chromatin configuration governing transcription regulation. To date, LSD1 has been identified in a number of corepressor complexes including CoREST (Lee et al., 2005; Shi et al., 2005), CtBP (Wang et al., 2007b) and a subset of HDAC complexes (You et al., 2001), and it has also been shown to interact with p53, repress p53-mediated transcription and inhibit p53-promoted apoptosis (Huang et al., 2007).

Despite progress in understanding the dynamic histone-methylation regulation and in revealing the diverse molecular interactions for LSD1, the biological function of LSD1 is just beginning to be uncovered. Although the histone demethylation/transcription regulation activity of LSD1 is potentially widespread, evidence suggests that LSD1 nevertheless performs pathway-specific functions (Di Stefano et al., 2007; Shi, 2007). In addition, recent studies have implicated LSD1 in several growth-promoting pathways and have linked LSD1 to certain high-risk tumors (Forneris et al., 2008; Kahl et al., 2006; Shi, 2007; Wang et al., 2007a). Indeed, within the framework of the so-called epigenetic therapies, there is a growing interest in LSD1 as a potential drug target (Shi, 2007).

Here we propose that LSD1 is an integral component of the Mi-2/nucleosome remodeling and deacetylase (NuRD) complex, adding histone demethylation activity to this complex. We show that LSD1/NuRD complexes regulate the metastatic potential of breast cancer cells and suppress breast cancer metastasis, implicating LSD1 in breast cancer metastasis.

RESULTS

LSD1 Is an Integral Component of the NuRD Complex

Molecular carcinogenesis has been the primary research focus in this laboratory (Shang, 2006; Shang and Brown, 2002; Shang et al., 2000; Shi et al., 2007; Wu et al., 2005; Yin et al., 2004). In an effort to better understand the mechanistic roles of the metastasis tumor antigen (MTA), a subunit of the NuRD complex (Bowen et al., 2004; Denslow and Wade, 2007; Fujita et al., 2003; Kumar et al., 2003), in cancer metastasis, we employed affinity purification and mass spectrometry to identify the proteins that are associated with MTA2, the phylogenetically closest relative to the ancestral MTA protein (Denslow and Wade, 2007; Manavathi and Kumar, 2007). In these experiments, FLAG-tagged MTA2 (FLAG-MTA2) was stably expressed in HeLa cells. Cellular extracts were prepared and subjected to affinity purification using an anti-FLAG affinity gel. Mass spectrometric analysis indicate that MTA2 copurified with Mi-2, HDAC1, HDAC2, RbAp46, RbAp48, and MBD3, all of which are components of the NuRD complex, as well as with LSD1 (Figure 1A). In addition, BRCA2 was also detected in the complex. The presence of LSD1 in the MTA2/NuRD complex was further confirmed

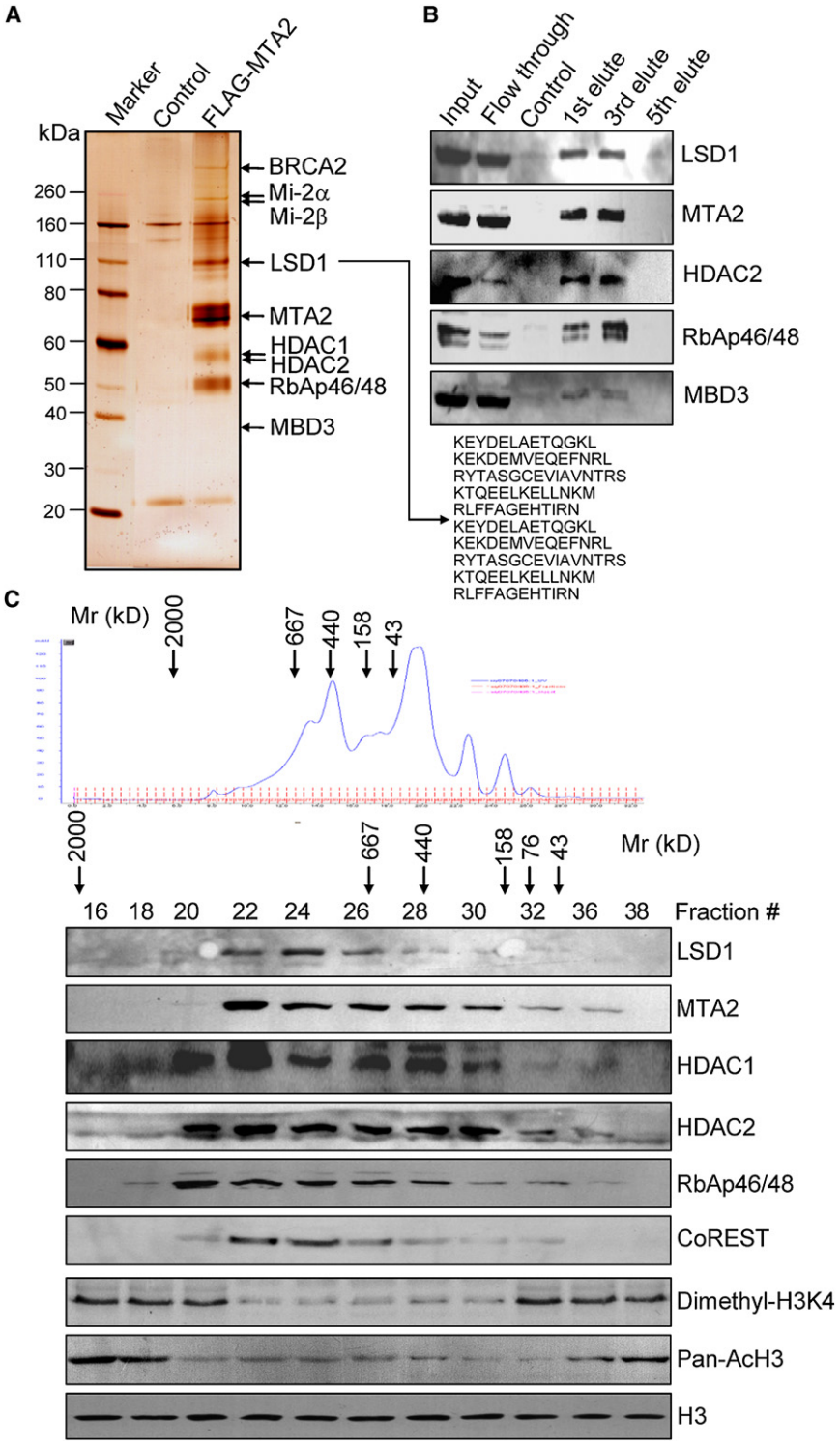

Figure 1. LSD1 Is Associated with the NuRD Complex

(A) Immunoaffinity purification of MTA2-containing protein complexes. Cellular extracts from HeLa cells stably expressing FLAG (control) or FLAG-MTA2 were immunopurified with anti-FLAG affinity columns and eluted with FLAG peptide. The eluates were resolved by SDS-PAGE and silver-stained. The proteins bands were retrieved and analyzed by mass spectrometry. Detailed results from the mass spectrometric analysis are provided in the Supplemental Data.

(B) Western blotting analysis of the identified proteins in the purified fractions using antibodies against the indicated proteins.

(C) Cofractionation of LSD1 and the NuRD complex by FPLC. Cellular extracts from HeLa cells were fractionated on Superose 6 size exclusion columns. Chromatographic elution profiles and immunoblotting analysis of the chromatographic fractions are shown. The elution positions of calibration proteins with known molecular masses (kDa) are indicated, and an equal volume from each fraction was analyzed.

with its antibodies by western blotting analysis (Figure 1B), suggesting that LSD1 is associated with the NuRD complex in vivo. The detailed results of the mass spectrometric analysis are provided in the Supplemental Data available with this article online.

To further show that LSD1 is associated with the NuRD complex in vivo, protein fractionation experiments were carried out by fast protein liquid chromatography (FPLC) with Superose 6 columns and a high salt extraction and size exclusion approach. Native LSD1 from HeLa cells was eluted with an apparent molecular mass much greater than that of the monomeric protein; LSD1 immunoreactivity was detected in chromatographic fractions from the Superose 6 column with a relatively symmetrical peak centered between ~669 and ~1000 kDa (Figure 1C). Significantly, the elution pattern of LSD1 largely overlapped with that of the NuRD complex proteins including MTA2, HDAC1, HDAC2, and RbAp46/48, further supporting the idea that LSD1 is associated with the NuRD complex in vivo. Moreover, the chromatographic profiles of the NuRD complex and LSD1 were compatible with their associated enzymatic activities. Specifically, histone deacetylation activity as well as histone demethylation activity was detected when the corresponding chromatographic fractions were incubated with calf thymus bulk histones and analyzed by western blotting with antibodies against acetyl-H3 and dimethyl-H3K4, respectively (Figure 1C, bottom three panels). Interestingly, the chromatographic profile of LSD1 was also overlapped with that of CoREST, suggesting that LSD1/NuRD complex and LSD1/CoREST complex coexist in HeLa cells.

To confirm the in vivo interaction between LSD1 and the NuRD complex, total proteins from HeLa cells were extracted, and coimmunoprecipitation experiments were performed with antibodies detecting the endogenous proteins. Immunoprecipitation (IP) with antibodies against LSD1 followed by immunoblotting (IB) with antibodies against Mi-2, HDAC1, HDAC2, MBD3, MTA1, MTA2, or MTA3 demonstrated that LSD1 coimmunoprecipitated with all of the NuRD components (Figure 2A, first column). Reciprocally, IP with antibodies against the components of the NuRD complex and IB with antibodies against LSD1 also revealed that the components of the NuRD complex coimmunoprecipitated with LSD1 (Figure 2A, second column). In addition, the association between LSD1 and the NuRD complex was also detected in human breast carcinoma MCF-7 cells (Figure 2B, first column) and MDA-MB-231 cells (Figure 2B, second column) when corresponding cellular extracts were immunoprecipitated with antibodies against LSD1 followed by immunoblotting with antibodies against Mi-2, HDAC1, HDAC2, MBD3, MTA1, MTA2, or MTA3.

To determine the relative amount of LSD1 associated with the NuRD complex versus that associated with CoREST in HeLa cells, equal amounts of HeLa cellular extracts were coimmunoprecipitated with antibodies against Mi-2 and CoREST, respectively. Immunoprecipitates were then immunoblotted with anti-LSD1. It is estimated that amount of LSD1 associated with the NuRD versus that associated with CoREST complex is 5:3 in HeLa cells (Figure 2C).

MTA2-Containing Complex Possesses Both Histone Demethylation and Deacetylation Activities

To further investigate the physical association and to examine the functional connection between LSD1 and the NuRD complex, the MTA2-containing protein complex was immunoprecipitated from HeLa cells stably expressing FLAG-MTA2 with the anti-FLAG antibody and analyzed for enzymatic activities. The immunoprecipitates (IPs) were first incubated either with bulk histones (Figure 3A) or with mononucleosomes (Figure 3B) isolated from HeLa cells, and the levels of methylated and acetylated histones in the reactions were then analyzed by western blotting. As expected, the MTA2-containing complex possessed an enzymatic activity that led to a significant decrease in the acetylation level of H3. Remarkably, however, the immunoprecipitates also contained a strong demethylase activity for di-methyl H3-K4 and an evident demethylase activity for mono-methyl H3-K4 on both bulk histones and the nucleosomal substrates, whereas no apparent effect on the di-methyl of H3-K9 was detected. Furthermore, the demethylation activity of the immunoprecipitates on di-methyl H3-K4 could be effectively inhibited by pargyline, an inhibitor specific for monoamine oxidases such as LSD1 (Figure 3C).

In vitro deacetylation and demethylation assays were also performed by incubating the immunoprecipitates with [^{3}H]methyl-labeled histone substrates or [^{3}H]acetate-labeled HeLa histones. The deacetylation and demethylation activity of the immunoprecipitates were measured by quantifying the release of radiolabeled acetyl groups or the formation of [^{3}H]-labeled formaldehyde from hyperacetylated HeLa histones or purified hypermethylated histone substrates, respectively. We found that the immunoprecipitates had histone deacetylation activity that could be effectively inhibited by trichostatin A (TSA), an HDAC inhibitor (Figure 3D, left). Additionally, the MTA2-containing complex also exhibited histone demethylase activity which could be effectively inhibited by pargyline (Figure 3D, right). Together with the

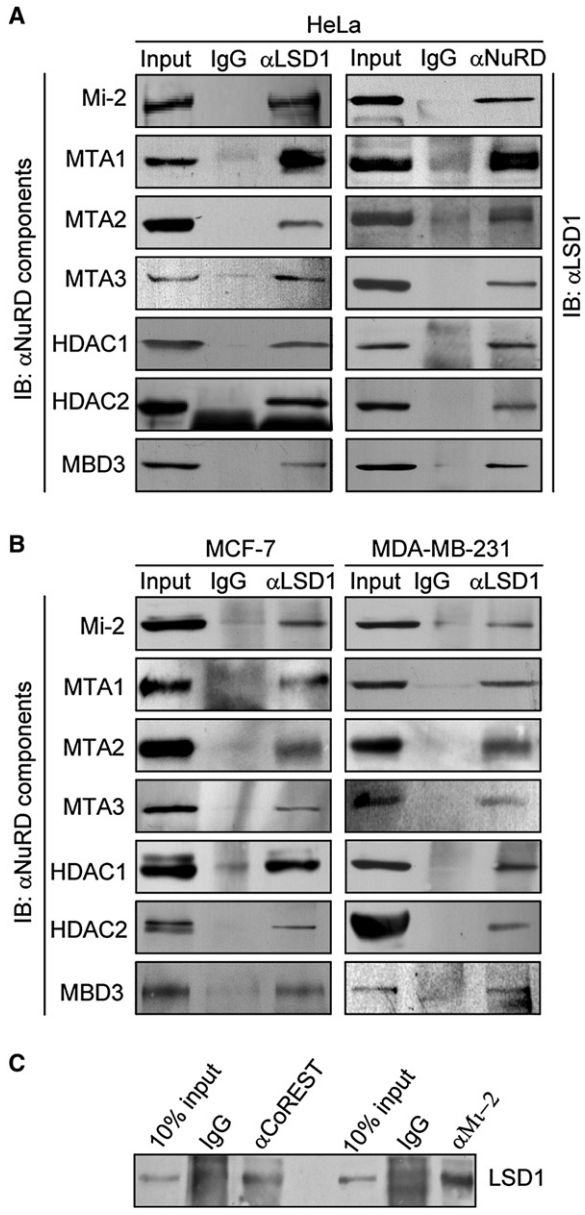

Figure 2. Physical Interaction between LSD1 and the NuRD Complex

(A) Association of LSD1 with the NuRD complex in HeLa cells. Whole cell lysates were immunoprecipitated (IP) with the antibodies against the indicated proteins. Immunocomplexes were then immunoblotted (IB) using antibodies against the indicated proteins.

(B) Association of LSD1 with the NuRD complex in MCF-7 and MDA-MB-231 cells.

(C) Equal amounts of HeLa cellular extracts were coimmunoprecipitated with antibodies against Mi-2 or CoREST, respectively. Immunoprecipitates were then immunoblotted with anti-LSD1.

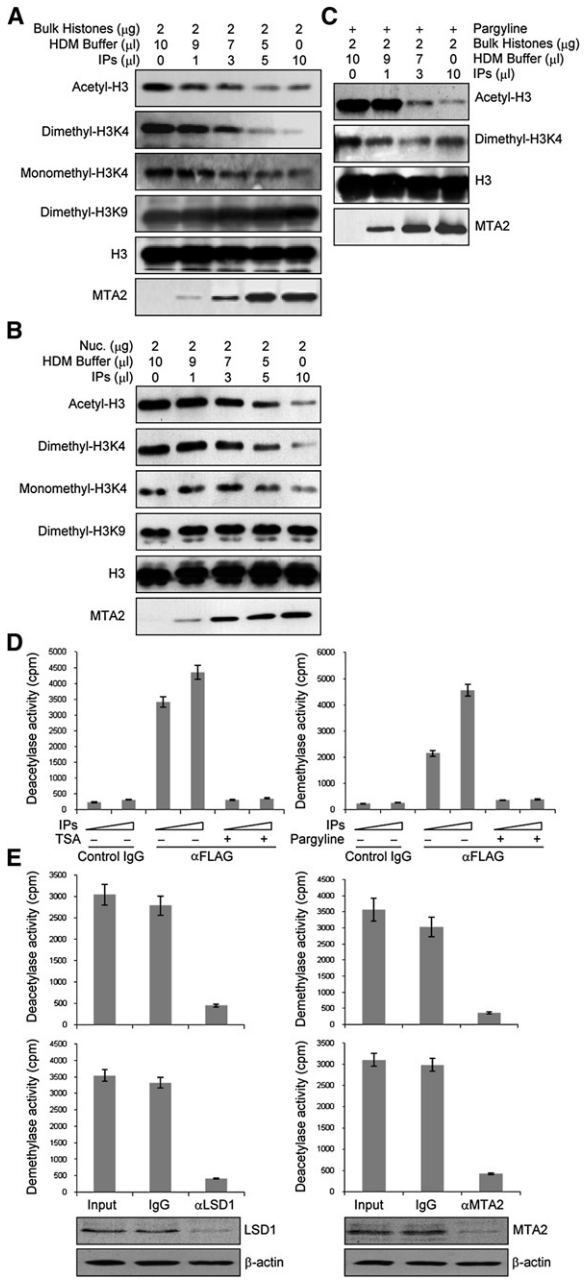

Figure 3. Functional Connection between LSD1 and the NuRD Complex

(A) The MTA2-containing protein complex possesses both histone demethylation and histone deacetylation activities. Cellular extracts were obtained from HeLa cells stably expressing FLAG-MTA2 and were immunoprecipitated with anti-FLAG antibody. The immunoprecipitates (IPs) were incubated with bulk histones and histone demethylation (HDM) or histone deacetylation (HDAC) assay buffer. The reaction mixtures were analyzed by western blotting using antibodies against the indicated histone marks or proteins. Acetyl-H3 represents acetyl-K9/K14 H3.

(B) The MTA2-containing protein complex can recognize nucleosomal substrates. Above-described IPs were incubated with mononucleosomes (Nucs) isolated from HeLa cells. The reaction mixtures were analyzed by western blotting using antibodies against the indicated histone marks or proteins.

(C) The histone demethylation activity of the MTA2-containing complex could be inhibited by pargyline. A similar experimental procedure as described for Figure 3A was followed with the addition of 1 mM of pargyline in the reactions.

(D) Histone demethylation and histone deacetylation activities of the MTA2-containing complex assayed with [^{3}H]acetate-labeled HeLa histones or [^{3}H]methyl-labeled histone substrates. The deacetylation and demethylation activities were measured by quantifying the release of radiolabeled acetyl groups or the formation of [^{3}H]-labeled formaldehyde, respectively, using liquid scintillation counting. Each bar represents the mean ± SD for triplicate measurements. cpm: counts per minute.

(E) Histone deacetylation and demethylation activities of the MTA2-containing complex assayed with [^{3}H]acetate-labeled HeLa histones or [^{3}H]methyl-labeled histone substrates after immunodepletion with antibodies against LSD1 or MTA2. Each bar represents the mean ± SD for triplicate measurements. The efficiency of the immunodepletion was examined by western blotting the supernatants with antibodies against LSD1 or MTA2.

enzymatic activity measurements conducted in fractionation experiments, these data indicate that the MTA2-containing complex possesses both histone deacetylation and demethylation activities.

In order to further support the idea that the demethylation activity and the deacetylation activity of the MTA2-containing complex are indeed physically associated, we performed immunodepletion assays in which the immunoprecipitates were incubated with anti-LSD1- or anti-MTA2-conjugated protein A/G-Sepharose beads. After two rounds of incubation and the removal of the resins by centrifugation, the supernatants were then used to perform deacetylase and demethylase assays with [^{3}H]-labeled HeLa cell histones or histone substrates. Immunodepletion of LSD1 resulted in a drastic decrease in the deacetylation activity (Figure 3E, upper left) and immunodepletion of MTA2 led to a significant loss in the demethylation activity of the MTA2-containing protein complex (Figure 3E, upper right). As control, LSD1-immunodepletion was associated with a diminished demethylation activity (Figure 3E, lower left) and MTA2-immunodepletion was accompanied by a decreased deacetylation activity (Figure 3E, lower right). These experiments strongly indicate that LSD1 and the NuRD complex are both physically and functionally associated, further supporting the idea that LSD1 is a subunit of the NuRD complex. The efficiency of the immunodepletion was examined by western blotting analysis of the supernatants (Figure 3E).

LSD1 Interacts Directly with MTA Proteins

In order to determine the molecular basis for the interaction of LSD1 with the NuRD complex, GST pull-down assays were conducted using GST-fused LSD1 construct and in vitro transcribed/translated individual components of the NuRD complex including MTA1, MTA2, MTA3, HDAC1, HDAC2, RbAp46, and RbAp48. These experiments revealed that LSD1 interacts directly with MTA1, MTA2 and MTA3, but not with the other components of the NuRD complex that we tested (Figure 4A).

LSD1 is an asymmetric molecule consisting of several distinct structural domains: the N-terminal putative nuclear localization signal followed by the SWIRM (Swi3, Rsc8, and Moira) domain; in the C terminus, there is a Tower domain that protrudes as an elongated helix-turn-helix motif out of the FAD-binding amine oxidase domain (AOD) (Cheng and Zhang, 2007; Forneris et al.,

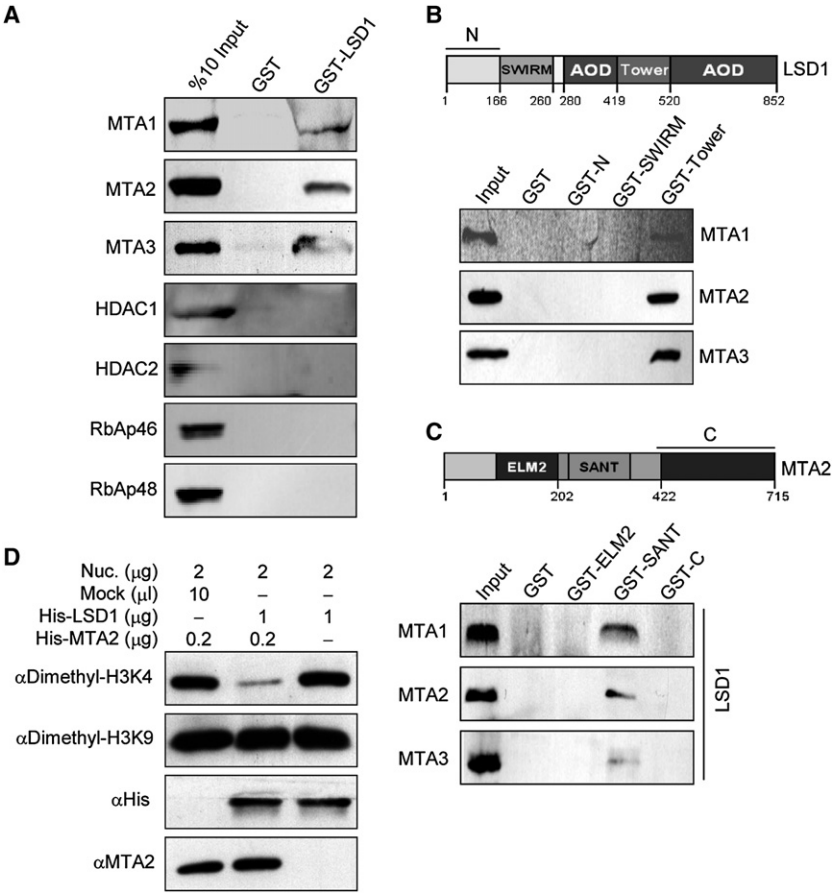

Figure 4. Molecular Interaction between LSD1 and the NuRD Complex

(A) GST pull-down experiments with bacterially expressed GST-LSD1 and the in vitro transcribed/translated indicated proteins.

(B) Mapping the interface in LSD1 for the interaction between LSD1 and MTAs by GST pull-down experiments with GST-fused LSD1 domain-constructs and in vitro transcribed/translated MTA1, MTA2, or MTA3.

(C) Mapping the interface in MTAs for the interaction between MTAs and LSD1 by GST pull-down experiments with GST-fused MTA domain-constructs and in vitro transcribed/translated LSD1.

(D) Requirement for MTA2 in the demethylation of nucleosomal substrate by LSD1. Mononucleosomes isolated from HeLa cells were used for demethylation reactions by His-LSD1 in the presence or absence of recombinant MTA2.

2008). In order to map the interaction interface of LSD1 with the members of the MTA family, GST pull-down assays were performed with a GST-fused LSD1 N-terminal fragment (1-166 aa), the SWIRM domain (167-260 aa), and the Tower domain (419-520 aa) and with in vitro transcribed/translated MTA1, MTA2, or MTA3. The results indicated that the Tower domain is responsible for the interaction of LSD1 with MTA1, MTA2, or MTA3 (Figure 4B). Analogously, mapping the interaction interface in MTAs with GST-fused MTA domain-constructs and in vitro transcribed/translated LSD1 revealed that the SANT (Swi3-Ada2-N-CoR-TFIIIB) domain of the MTA proteins is responsible for the interaction of MTAs with LSD1 (Figure 4C).

It has been reported that bacterially purified LSD1 can demethylate mono- or dimethylated H3K4 only when the substrate is either a histone peptide or free histone; recombinant LSD1 was unable to demethylate nucleosomal substrates (Shi et al., 2004, 2005). It has also been demonstrated that nucleosomal substrate recognition by LSD1 requires proteins like CoREST (Shi et al., 2005) that possess a histone-tail-presenting module, such as the SANT domain, to bridge LSD1 to the chromatin structure. The interaction of LSD1 with the MTA proteins and the presence of the SANT domain in these proteins suggest that the MTA proteins may act as bridging factors in the NuRD complex for LSD1 to act on nucleosomes. In order to investigate this hypothesis, we performed histone demethylation assays on isolated mononucleosomes. As shown in Figure 4D, while recombinant LSD1 alone was unable to demethylate H3K4, addition of MTA2 to the demethylation reaction endowed the ability of recombinant LSD1 to demethylate nucleosomal substrates, supporting the idea that the MTA proteins in the NuRD complex function to bridge LSD1 to the chromatin structure.

Transcription Target Analysis for LSD1/NuRD Complexes

As mentioned earlier, both LSD1 and the NuRD complex are mainly implicated in gene transcription repression through their catalytic activities impacting the chromatin configuration. In order to further investigate the functional association between LSD1 and the NuRD complex and to explore the biological significance of this association, we analyzed the genome-wide transcriptional targets of the LSD1/NuRD complexes using the Chromatin ImmunoPrecipitation-DNA Selection and Ligation (ChIP-DSL) approach. It is believed that the individual members of the MTA family constitute distinct forms of the NuRD complex (Bowen et al., 2004; Denslow and Wade, 2007). Given our observation that LSD1 is capable of interacting with all three members of the MTA family, we designed the ChIP-DSL experiments based on the assumption that LSD1/NuRD complexes include LSD1/MTA1/NuRD, LSD1/MTA2/NuRD, and LSD1/MTA3/NuRD complexes. In these experiments, ChIP experiments were conducted in MCF-7 cells with antibodies against LSD1, MTA1, MTA2, or MTA3. Following ChIP, LSD1- and MTA-associated DNAs were amplified using nonbiased conditions, labeled, and hybridized to AVIVA Hu20K arrays. Relative confidence prediction scores were generated by quantile normalization across each probe followed by an analysis using a two-state Hidden Markov model (Mukherjee and Mitra, 2005). These scores included both probe intensity and width of probe cluster. Triplicate experiments were performed to eliminate stochastic false positives, after which peaks that reproducibly appeared at least twice in the three replicates were included. The data from LSD1 antibodies were then

analyzed with the data from antibodies against each individual MTA protein for overlapping promoters, and these promoters were considered to be the targets of the LSD1/MTA1/NuRD, LSD1/MTA2/NuRD, and LSD1/MTA3/NuRD complexes (Figure 5A). Collectively, all targets were considered to be targets of the LSD1/NuRD complexes. These experiments identified a total of 1,153 different promoters targeted by the LSD1/NuRD complexes. Of these, 725 were targeted by the LSD1/MTA1/NuRD complex, 716 by the LSD1/MTA2/NuRD complex, and 631 by the LSD1/MTA3/NuRD complex (Figure 5A). Among them, 252 promoters were identified as common targets for LSD1/MTA1/NuRD, LSD1/MTA2/NuRD, and LSD1/MTA3/NuRD. These data indicate that different LSD1/MTA/NuRD complexes target distinct yet overlapping sets of genes. The detailed results of the ChIP-DSL experiments are deposited in GEO Datasets (accession ID: GSE14260) and summarized in the Supplemental Data Excel spreadsheet.

The genes that are regulated by these promoters were then classified into cellular signaling pathways for each individual LSD1/MTA/NuRD complex as well as for all three complexes combined using MAS software (http://bioinfo.capitalbio.com/mas) with a p value cutoff of 10^{-3}. These analyses revealed again that different LSD1/MTA/NuRD complexes target distinct yet overlapping signaling pathways (Figure 5A, red rectangles). Interestingly, analysis of the combined targets of the LSD1/MTA1/NuRD, LSD1/MTA2/NuRD, and LSD1/MTA3/NuRD complexes identified signaling pathways including TGFβ, cell communication, focal adhesion, MAPK, and cell cycle that are critically involved in cell growth, survival, migration, and invasion. The genes in these pathways include, among others, *TGFB1*, *EGFR*, *RHOA*, *ANGPTL4*, *LAMININ ALPHA 4, COLLAGEN VI* and *ENDOTHELIN-1* that are known to be implicated in epithelial-to-mesenchymal transition and/or metastasis.

Real-time quantitative RT-PCR analysis in MCF-7 cells under LSD1 knockdown of the mRNA expression of selected genes, including *TGFB1*, *LMNB2*, *IGF1R*, *EGFR*, *CCND1*, *ADK*, *PSEN1*, *RHOA*, *FGF21*, *and APAF1*, which represent each of the pathways, confirmed the ChIP-DSL experiments (Figure 5B, upper panel). Moreover, in LSD1-overexpressing MCF-7 cells, knocking down the expression of MTA1 but not MTA2 or MTA3 rendered the lost repression of *IGF1R*, which was identified as a target of the LSD1/MTA1/NuRD complex in ChIP-DSL experiments, and knocking down the expression of MTA2 but not MTA1 or MTA3 led to a relieved repression of *RHOA*, which was identified as a target of the LSD1/MTA2/NuRD complex in ChIP-DSL experiments (Figure 5B, lower panel). These observations further validated the results from the ChIP-DSL experiments and support the idea that LSD1 forms distinct NuRD complexes. The ChIP-DSL experiments were further substantiated by conventional ChIP to demonstrate that LSD1 and MTA3 co-occupy the *TGFB1* promoter in MCF-7 cells (Figure 5C). In addition, sequential ChIP or ChIP/Re-ChIP (Shang et al., 2000; Zhang et al., 2004) confirmed that LSD1, MTA3, and Mi-2 exist in the same protein complex on the *TGFB1* promoter (Figure 5C). Taken together, these experiments not only support the idea that *TGFB1* is targeted by the LSD1/MTA3/NuRD complex but also confirm that LSD1 is physically associated with and is an integral component of the NuRD complex in vivo.

LSD1 Inhibits Breast Cancer Cell Invasion In Vitro

The identification of the key regulators in epithelial-to-mesenchymal transitions, such as TGFβ1 (Yang and Weinberg, 2008; Zavadil and Bottinger, 2005), as targets of LSD1/NuRD complexes and the well-documented roles of TGFβ1 in breast cancer metastasis (Massague, 2008; Massague et al., 2000; Padua et al., 2008; Welch et al., 1990; Yang et al., 2008) suggest that LSD1 may also function in breast cancer invasion and metastasis. Therefore, we first investigated the effect of LSD1 on the cellular behavior of breast cancer cells in vitro. For this purpose, LSD1 was overexpressed or knocked down in MDA-MB-231 cells via lentiviral infection, and the impact of the gain-of-function and loss-of-function of LSD1 on the invasive potential of these cells was investigated using transwell invasion assays. These experiments show that while overexpression of wild-type LSD1 resulted in more than 3-fold decrease in cell invasion, overexpression of the Tower domain-deleted LSD1 mutant had little effect on cell invasion (Figure 6A). This is consistent with our observation that LSD1 is incorporated into the NuRD complex through its interaction with this domain with MTA proteins. On the other hand, LSD1 knockdown led to increased cell invasion about 5-fold (Figure 6A). In addition, the effect of LSD1 on the invasive potential of MDA-MB-231 cells was probably through the association of LSD1 with the NuRD complex, as overexpression of LSD1 but knockdown of the expression of Mi-2 resulted in a diminished LSD1 effect (Figure 6A). Moreover, the inhibitory effect of LSD1 overexpression on the invasive potential of MDA-MB-231 cells could be rescued by addition of exogenous TGFβ1 (Figure 6B) and the invasion-promoting effect of LSD1 knockdown could be effectively inhibited by SB-431542, an ATP analog inhibitor of the TGFβ type I receptor kinase (Laping et al., 2002) (Figure 6C). The activation of the TGFβ1 signaling by exogenous TGFβ1 and inhibition of the TGFβ1 signaling by SB-431542 in MDA-MB-231 cells were examined by western blotting analysis of the phosphorylation of SMAD3 and the expression of fibronectin (Figures 6B and 6C, right panels). These results suggest a critical role of the TGFβ1 signaling pathway in mediating the effect of LSD1 on the invasive potential of MDA-MB-231 cells.

LSD1 Suppresses Breast Cancer Metastatic Potential In Vivo

In order to further study the invasion-inhibitory effect of LSD1 and to investigate its possible role in breast cancer metastasis in vivo, MDA-MB-231 cells that had been engineered to stably express firefly luciferase (MDA-MB-231-Luc-D3H2LN, Xenogen Corporation) were infected with lentivirues carrying LSD1 cDNA or LSD1-specific siRNA. The effect of the gain-of-function and loss-of-function of LSD1 on spontaneous lung metastasis, on seeding lung metastasis, and on seeding bone metastasis of MDA-MB-231-Luc-D3H2LN tumors was assessed in immunocompromised SCID mice by orthotopic implantation, intravenous injection, and intracardiac injection, respectively. In these experiments, MDA-MB-231-Luc-D3H2LN cells were either implanted into the abdominal mammary fat pad (n = 10), or injected into the lateral tail vein (n = 8) or the left ventricle (n = 8) of 6-week old female SCID mice. The growth/dissemination of tumors was monitored weekly by bioluminescence imaging with IVIS imaging

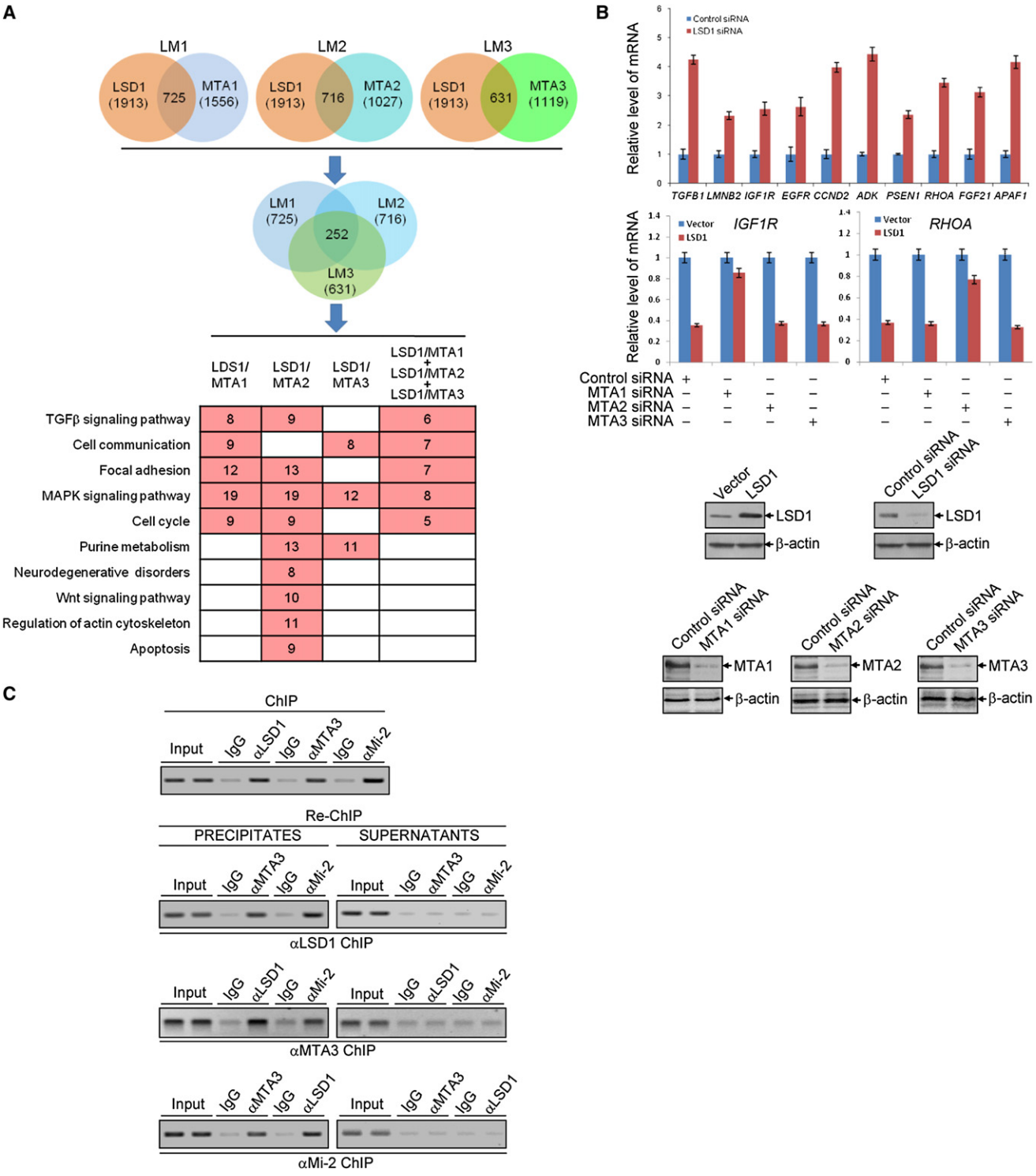

Figure 5. Transcription Target Analysis for LSD1/NuRD Complexes

(A) The experimental scheme and the working model for the ChIP-DSL experiments for the identification of transcriptional targets for LSD1/NuRD complexes in MCF-7 cells. The numbers represent the number of the promoters that were targeted by the indicated proteins and that appeared at least twice in triplicate experiments. The genes that are regulated by the identified promoters were classified into cellular signaling pathways with MAS software (http://bioinfo.capitalbio.com/mas) with a p value less than 10^{-3} and are highlighted with red color. The numbers in the red rectangles represent the number of corresponding pathway-related genes. The detailed results of the ChIP-DSL experiments are provided in the Supplemental Data Excel spreadsheet.

system (Xenogen Corporation). Tumor metastasis was measured by quantitative bioluminescence imaging after 7 weeks for orthotopically implanted groups. For intravenous injection groups or the intracardiac injection groups, the quantitative bioluminescence imaging was performed at 6 weeks or 4 weeks, respectively, after injection. We defined a metastatic event as any detectable luciferase signal above background and away from the primary tumor site. The results showed that, in orthotopically implanted groups, while either LSD1 overexpression or knockdown did not affect the ability of MDA-MB-231-Luc-D3H2LN cells to grow as mammary tumors and to pass into the circulation, the spontaneous lung metastasis was suppressed in animals carrying MDA-MB-231-Luc-D3H2LN tumors with LSD1 overexpression and was enhanced in animals carrying MDA-MB-231-Luc-D3H2LN tumors with LSD1 knockdown, as measured by bioluminescence imaging quantifying the photon flux (Figure 7A). In the intravenous injection groups, significant decreases in lung metastasis of tumor cells were observed in animals injected with MDA-MB-231-Luc-D3H2LN cells with LSD1 overexpression and significant increases in lung metastasis of tumor cells were recorded in animals injected with MDA-MB-231-Luc-D3H2LN cells with LSD1 knockdown (Figure 7B). Similarly, the bone metastasis seeding of tumor cells was significantly decreased when LSD1 was overexpressed and was greatly enhanced when LSD1 was knocked down in the intracardiac injection groups (Figure 7C). The metastases to lung and bone were verified by histological staining/immunostaining and X-ray examination, respectively. These experiments indicate that LSD1 overexpression suppressed the metastatic spread of MDA-MB-231-Luc-D3H2LN tumors and LSD1 knockdown enhanced the metastatic spread of the tumors in SCID mice, suggesting that LSD1 suppresses the metastatic potential of breast cancer in vivo.

LSD1 Is Downregulated in Breast Carcinomas and Its Level of Expression Is Negatively Correlated with that of *TGFB1*

In order to further support the role of LSD1 in breast cancer as well as to substantiate the functional link between LSD1 and TGFβ1 and extend the physiological relevance of this link, we collected 65 breast tumor samples, of which 30 included adjacent normal tissue, from breast cancer patients. The expression of *LSD1* and *TGFB1* mRNAs was analyzed by real time RT-PCR with *GAPDH* as the internal control. The results revealed a statistically significant decrease in *LSD1* expression in tumors compared to the adjacent normal mammary tissue (two-tailed paired t test, $n = 30$, $p = 0.0002$). In addition, statistical analysis found a Spearman correlation coefficient of -0.5535 ($p < 0.0001$) and a Pearson correlation coefficient of -0.5335 ($p < 0.0001$) when the relative level of *TGFB1*expression was plotted against the relative level of *LSD1* expression in breast carcinoma samples ($n = 65$), indicating a significant negative correlation between *LSD1* and *TGFB1* expression in these samples. These data are consistent with a role of LSD1 in suppressing breast cancer metastasis and support TGFβ1 as a downstream effector of LSD1.

DISCUSSION

Both LSD1 and the NuRD complex primarily function in transcription repression programs by virtue of their enzymatic activities and through their chromatin remodeling capabilities. Specifically, LSD1 targets H3-K4 for demethylation and the NuRD complex possesses histone deacetylation activity. As both demethylation and deacetylation are essential epigenetic mechanisms in controlling gene transcription, interplay between deacetylation and demethylation is a logical scenario. Indeed, past studies have indicated that histone deacetylation and demethylation are interdependent (Denslow and Wade, 2007; Lee et al., 2006; Shi et al., 2005). We propose that LSD1 is an integral component of the NuRD complex, placing deacetylase and demethylase activities into the same protein complex. By enlisting LSD1, the NuRD complex arsenal would include ATPase, deacetylase, and demethylase. The question then is: what is the biological significance of having all of these enzymatic activities in one single assembly? As stated above, these enzymatic activities are part of the whole pact of epigenetic actions that are necessary to bring a gene to a silenced state. Therefore, it is conceivable that evolution favors a physical proximity for more efficient functional interaction of distinct enzymatic activities. Such a stoichiometry would benefit for an exquisite coordination of distinct chromatin remodeling activities in finely-tuned gene regulation. In fact, in addition to these chromatin modification capacities, the NuRD complex also contains MBD2/MBD3, a protein that is connected to DNA methylation, another epigenetic mechanism in gene regulation. It is not expected that the NuRD complex contains all types of epigenetic modifiers, but it will not be surprising if future investigations uncover additional enzymatic activities that are associated with this complex, especially considering the dynamic nature of the assembly and functioning of this complex. In addition, as H3-K4 methylation encodes for a well-recognized epigenetic message signaling gene activation, it is logical to imagine that the repression function of the NuRD complex contains an enzymatic activity to erase this mark. Moreover, it is believed that at least one of the mechanistic manifestations for functional specificity of different forms of the NuRD complex is to be recruited by different transcription factors. To date, the NuRD complex has been shown to mediate transcription repression by distinct sequence-specific transcription factors including p53, Ikaros, Hunchback, Tramtrack69, KAP-1, BCL-6, and FOG-1 (Denslow and Wade, 2007). Interestingly, at least some of these transcription factors, such as p53, Ikaros, and Tramtrack88, also recruit LSD1 (Lan et al., 2008), again favoring a model in which LSD1 and the NuRD complex act together. More importantly, evidence

(B) Verification of the ChIP-DSL results by real-time RT-PCR analysis of mRNA expression of the indicated genes in MCF-7 cells after transfection with LSD1 expression vector, control siRNA, or siRNAs targeting MTA1, MTA2, or MTA3 as indicated. Each bar represents the mean ± SD for triplicate measurements. The effect of RNAi on protein expression was examined by western blotting with antibodies against the indicated proteins.

(C) LSD1 and the NuRD complex exist in the same protein complex on the *TGFB1* promoter. ChIP and Re-ChIP experiments were performed in MCF-7 cells with the indicated antibodies.

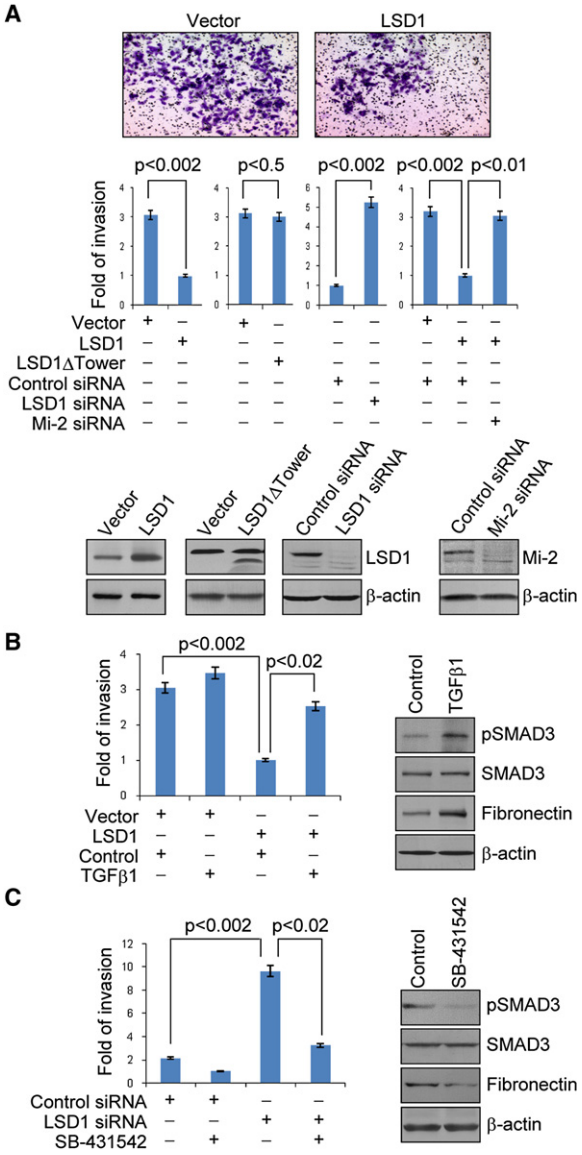

Figure 6. LSD1 Inhibits the Invasive Potential of MDA-MB-231 Cells In Vitro

(A) MDA-MB-231 cells were infected with lentiviruses carrying either empty vector, LSD1 expression vector, LSD1ΔTower, control siRNA, or LSD1 siRNA, or transfected with Mi-2 siRNA as indicated. The cells were starved for 18 h before cell invasion assays were performed using Matrigel transwell filters. The invaded cells were stained and counted. The images represent one field under microscopy in control (vector) and LSD1-overexpressing (LSD1) groups, respectively. Each bar represents the mean ± SD for triplicate measurements. The protein expression in these experiments was examined by western blotting using antibodies against the indicated proteins.

(B) Exogenous TGFβ1 alleviated the invasion-inhibitory effect of LSD1 overexpression. Cell invasion assays were performed in MDA-MB-231 cells under overexpression of LSD1 and the treatment with 100 pM of TGFβ1. The invaded cells were stained and counted. Each bar represents the mean ± SD for triplicate measurements. The activation of TGFβ1 signaling pathway in these cells by exogenous TGFβ1 was examined by western blotting analysis of the level of phosphorylated SMAD3 (pSMAD3), total SMAD3, and fibronectin, a downstream target of the TGFβ1 signaling pathway.

(C) Inhibition of TGFβ1 signaling by SB-431542 suppressed the invasion-promoting effect of LSD1 knockdown. Cell invasion assays were performed in MDA-MB-231 cells under knockdown of LSD1 and treatment with 10 μM of SB-431542. The invaded cells were stained and counted. Each bar represents the mean ± SD for triplicate measurements. The inhibition of TGFβ1 signaling by SB-431542 in MDA-MB-231 cells was confirmed by western blotting analysis of the level of phosphorylated SMAD3 (pSMAD3), total SMAD3, and fibronectin.

clearly points to a convergent role of LSD1 and the NuRD complex in cell fate determination and differentiation (Bowen et al., 2004; Shi, 2007), supporting a physical association and thus a functional connection between LSD1 and the NuRD complex. It is conceivable that LSD1, through being incorporated into and forming distinct NuRD complexes, is recruited by distinct pathway-specific transcription factors to exert its pathway-specific functions.

LSD1 has been implicated in cellular growth pathways and it has been linked with several types of cancer (Kahl et al., 2006; Wang et al., 2007a). Our experiments demonstrated, by both gain-of-function and loss-of-function studies, that LSD1 had dramatic effects on the metastatic behavior of MDA-MB-231 cells. ChIP-DSL analyses revealed that the LSD1/NuRD complexes target the promoters of an array of genes that constitute several important cellular signaling pathways pertinent to cell growth, survival, migration, and invasion. These include the TGFβ signaling pathway that is critically involved in epithelial-mesenchymal transitions and tumor invasion. Because epithelial-mesenchymal transition and metastasis are such hallmark events in morphogenesis and cell survival, the connection of LSD1 with these cellular behaviors emphasizes the importance of LSD1 in normal physiology and pathobiology. This is underscored by the observation that *LSD1* ablation causes embryonic lethality in mice (Wang et al., 2007b). On the other hand, as important as the epithelial-mesenchymal transition and metastasis are, it is logical to believe that only well-coordinated and sophisticated molecular machineries would make these missions possible. The association of LSD1 with the NuRD complex and the formation of different LSD1/NuRD complexes may thus provide at least a clue about the role of LSD1 in this sophisticated coordination. It is reasonable to believe that the aforementioned cell fate determination and differentiation function of LSD1 and the NuRD complex are due at least in part to the concerted networking of different forms of the LSD1/NuRD complexes. These functions represent the cellular readouts of the coordinated molecular actions of these complexes in normal development and in tumor invasion.

Our data indicate that modulating the expression of LSD1 did not affect the ability of MDA-MB-231 cells to grow as mammary tumors or to pass into the circulation in animals but did influence the invasive potential in cell culture. The reason for this discrepancy is not clear. But it is reasonable to expect a certain degree of difference between the behavior of the cells in vitro and in vivo.

TGFβ1 is a key player in epithelial-mesenchymal transitions and tumor invasion (Dumont and Arteaga, 2003; Massague, 2008; Massague et al., 2000; Siegel and Massague, 2003; Thiery, 2002). In fact, a recent study indicated that TGFβ1 could prime and empower breast cancer cells for metastasis to the lungs (Padua et al., 2008). Therefore, the regulation of TGFβ1 by

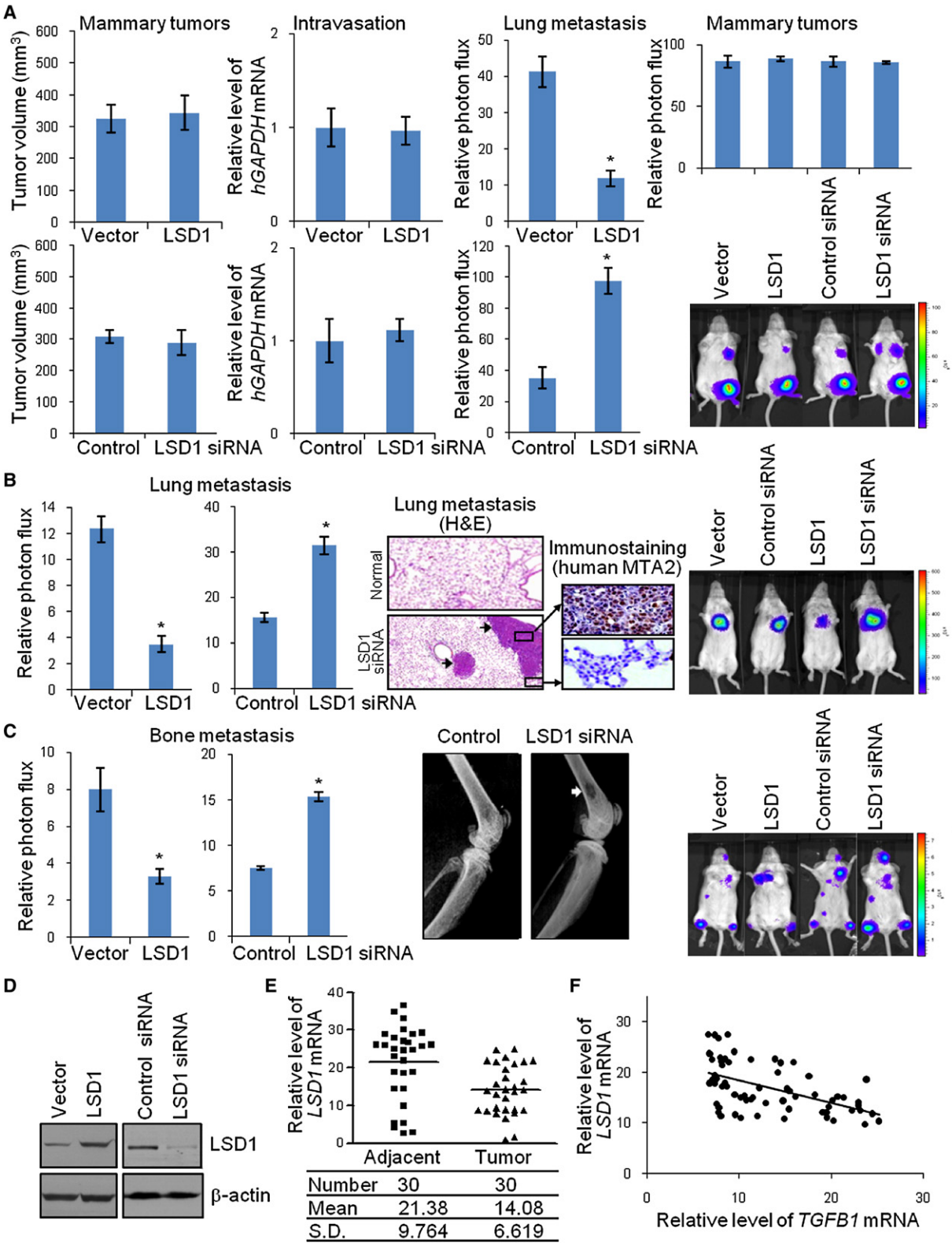

Figure 7. LSD1 Suppresses Breast Cancer Metastatic Potential In Vivo

(A) The effect of LSD1 on spontaneous lung metastasis of orthotopic breast cancer cells. MDA-MB-231-Luc-D3H2LN cells were infected with lentiviruses carrying either empty vector (vector), LSD1 expression construct (LSD1), control siRNA (control), or LSD1 siRNA, and were inoculated orthotopically into the

LSD1/NuRD complexes may have significant physiological implications. In agreement with this notion, we found that LSD1 suppresses breast cancer metastatic potential in vivo. We also showed that LSD1 expression was significantly lower in tumor samples compared to adjacent normal tissue and that the level of LSD1 expression was negatively correlated with the level of TGFβ1 expression. These results support a model in which at least one of the cellular functions of LSD1 is to incorporate into the NuRD complex and to target the epithelial-mesenchymal transition and tumor metastatic programs including the TGFβ signaling pathway. This proposition is consistent with reports by others that above-mentioned LSD1/NuRD-recruiting transcription factors, such as p53 (Sasai et al., 2008) and Hunchback (Yamazaki et al., 2006), target TGFβ signaling.

It remains to be investigated the functional association of LSD1 with the NuRD complex in normal development and physiology. Also relevant to our observations, it will be important to determine the molecular basis underlying differential promoter recognition by the different forms of the LSD1/NuRD complex and to explore the mechanism by which the coordinated actions of distinct LSD1/NuRD complexes are achieved in the epithelial-mesenchymal transition in normal development and to investigate how this coordination might be altered in tumor metastasis. Interestingly, our experiments identified BRCA2 in LSD1/NuRD complexes. The significance of this association needs further investigation. Relevant to this, ChIP-DSL identified *BRCA2* as a common target of the LSD1/NuRD complexes; also *CHD4* (Mi-2β) was identified as a target for the LSD1/MTA1/NuRD complex and MTA3 itself was identified as a target for the LSD1/MTA3/NuRD complex. Whether feedback regulatory loops exist for the LSD1/NuRD complexes and what role(s) this mechanism might contribute to the coordinated actions of different forms of LSD1/NuRD complexes need to be determined. Nevertheless, if our interpretation is correct, our experiments indicate that LSD1 is a bona fide subunit of the NuRD complex, expanding the enzymatic repertoire of the NuRD complex in epigenetic regulation and providing a molecular basis for the interdependence of histone deacetylation and demethylation in chromatin remodeling. We showed that LSD1 represses the transcription of a number of important cellular regulators and suppresses breast cancer metastasis, supporting the pursuit of LSD1 as a target for cancer therapy.

EXPERIMENTAL PROCEDURES

Immunopurification and Mass Spectrometry

Lysates from HeLa cells stably expressing FLAG-MTA2 were applied to an equilibrated FLAG column. The column was then washed and the protein complex was eluted with FLAG peptides (Sigma). Fractions of the bed volume were collected and resolved on SDS-PAGE, silver stained, and subjected to LC-MS/MS sequencing and data analysis.

FPLC Chromatography

HeLa nuclear extracts were applied to a Superose 6 size exclusion column (Amersham Biosciences) that had been equilibrated with dithiothreitol-containing buffer and calibrated with protein standards (blue dextran, 2000 kDa; thyroglobulin, 669 kDa; ferritin, 440 kDa; catalase, 232 kDa; bovine serum albumin, 67 kDa; and RNase A, 13.7 kDa; all from Amersham Biosciences). The column was eluted at a flow rate of 0.5 ml/min and fractions were collected.

Demethylation and Deacetylation Assays

Calf thymus bulk histones (Sigma) were incubated with MTA2-containing complex in histone demethylase assay buffer. The reaction mixture was analyzed by western blotting against di- or mono-methyl-H3K4, di-methyl-H3K9, acetyl-H3K9/K14, and H3 N-terminal tail. For radiolabeled demethylation assays, [^{3}H]methyl-labeled histone substrates were prepared and incubated with the MTA2-containing complex. The radioactivity was measured by liquid scintillation counting. For radiolabeled deacetylation assays, protein fractions were incubated with [^{3}H]acetate-labeled HeLa histones that had been isolated from butyrate-treated HeLa cells. The released [^{3}H]acetate was extracted with ethyl acetate and quantified by liquid scintillation counting.

Immunoprecipitation and Immunodepletion

For immunoprecipitation assays, cellular extracts were incubated with appropriate primary antibodies or normal rabbit/mouse immunoglobin G (IgG) at 4°C overnight, followed by addition of protein A/G Sepharose CL-4B beads for 2 hr at 4°C. Beads were then washed and the immune complexes were subjected to SDS-PAGE followed by immunoblotting with secondary antibodies. Immunodetection was performed using enhanced chemiluminescence (ECL System, Amersham Biosciences) according to the manufacturer's instructions. For immunodepletion assays, preimmune serum or specific antibodies were first immobilized to protein A/G-Sepharose. HeLa immunoprecipitates were incubated with antibody-conjugated protein A/G-Sepharose beads for 2 hr at 4°C. The precipitates were removed by centrifugation, and the supernatants were subjected to a second round of immunodepletion with protein A/G-Sepharose resins freshly preadsorbed with corresponding antibodies. After removing the resins by centrifugation, the supernatants were transferred to new tubes and stored at −70°C until used.

abdominal mammary fat pad of 6-week-old female SCID mice (n = 10). Tumor size was measured on day 28 (mammary tumors, n = 6). The presence of circulating tumor cells (intravasation, n = 3) was assessed by real time RT-PCR as a function of human *GAPDH* expression relative to murine *β2-microglobulin* in 3 ml of mouse blood perfusate. Primary tumors and lung metastases were quantified using bioluminescence imaging (n = 5-6) after 7 weeks of initial implantation. Error bars indicate mean ± SD; *p < 0.002 (two-tailed paired t test). Representative in vivo bioluminescent images are shown.

(B) The effect of LSD1 on seeding lung metastasis of intravenously injected breast cancer cells. The above described MDA-MB-231-Luc-D3H2LN cells were injected intravenously through the tail vein of 6-week-old female SCID mice (n = 8). Lung metastasis was quantified using bioluminescence imaging after 6 weeks (n = 6–8). Error bars indicate mean ± SD; *p < 0.01 (two-tailed paired t test). Lung sections from normal (untreated) or LSD1 siRNA-treated mice were stained with H&E or were immunostained with antibodies specific for human MTA2 (Abcam, ab9949) (middle). Representative in vivo bioluminescent images are shown (right).

(C) The effect of LSD1 on seeding bone metastasis of intracardiacally injected breast cancer cells. The above described MDA-MB-231-Luc-D3H2LN cells were injected into the left ventricle of female SCID mice (n = 8). Bone metastasis was quantified after 4 weeks using bioluminescence imaging of the mouse hindlimbs (n = 6). Error bars indicate mean ± SD; *p < 0.01 (two-tailed paired t test). Representative mouse hindlimb radiographs (middle; white arrows indicate metastases) from control siRNA (control)- or LSD1 siRNA-treated mice and bioluminescent images (right) are shown.

(D) Confirmation of LSD1 overexpression and knockdown in MDA-MB-231-Luc-D3H2LN cells used in animal experiments by western blotting.

(E) LSD1 is downregulated in breast carcinomas. Paired breast tumor samples versus adjacent normal tissue (n = 30) were analyzed by real time RT-PCR for the expression of *LSD1* mRNA with *GAPDH* as the reference.

(F) The level of *LSD1* mRNA expression in breast carcinomas is negatively correlated with that of *TGFB1*. The expression of *LSD1* and *TGFB1* mRNAs was analyzed by real time RT-PCR in 65 breast carcinoma samples with *GAPDH* as the reference. The relative level of *TGFB1*expression was plotted against the relative level of *LSD1* expression.

ChIP-DSL

ChIP samples were amplified by ligation-mediated PCR as described (Kwon et al., 2007). DNA fragmentation, biotin labeling, and hybridization were performed according to a protocol from Aviva Systems Biology (http://www.avivasysbio.com) using Aviva Hu20K arrays. Experiments were repeated three times and the results were analyzed using MAS (http://bioinfo.capitalbio.com/mas/login.do) with a p value cutoff of 1.0×10^{-6} for promoter identification and $p < 0.001$ for pathway analysis.

ChIP and Re-ChIP

ChIP and Re-ChIP were performed in MDA-MB-231 cells as described previously (Zhang et al., 2006; Zhang et al., 2004; Zhang et al., 2007). The enrichment of the DNA template was analyzed by conventional PCR using primers: forward: 5′-GATGGCACAGTGGTCAAGAGC-3′ and reverse: 5′-GAAGGATG GAAGGGTCAGGAG-3′ specific for TGFB1 gene promoter.

Lentiviral Production and Infection

Recombinant lentiviruses were constructed by subcloning human LSD1 into the iDuet101 shuttle vector (Ye et al., 2008). The recombinant construct as well as two assistant vectors: cytomegalovirus (CMV) R8.91 and pMD.G, were then transiently transfected into HEK293T cells. Viral supernatants were collected, filtered, concentrated, and used to infect cells. The construction of RNAi lentivirus system using pLL3.7 and other LentiLox vectors was carried out according to a protocol described online (http://web.mit.edu/jacks-lab/protocols/lentiviralproduction.htm). In brief, siRNA sequences targeting LSD1 were designed and cloned into the pLL3.7 shuttle vector. The recombinant construct, as well as three assistant vectors: pMDLg/pRRE, pRSV-REV, and pVSUG, were then transiently transfected into HEK293T cells. Viral supernatants were collected 48 h later, clarified by filtration, and concentrated by ultracentrifugation. The concentrated virus was used to infect 5×10^5 cells in a 60 mm dish with 8 μg/ml polybrene. Infected MDA-MB-231 cells were then subjected to sorting by EGFP expression.

Cell Invasion Assay

Transwell chamber filters (Chemicon Incorporation) were coated with Matrigel. After infection with lentivirus, MDA-MB-231 cells were starved for 18 hr in DMEM containing 0.1% BSA, and 1.5×10^5 of cells in 300 μl serum free media were placed to the upper chamber of the transwell. The chamber was then transferred to a well containing 500 μl of media containing 10% fetal bovine serum. Cells were incubated for 24 hr at 37°C. Cells in the top well were removed by wiping the top of the membrane with cotton swabs. The membranes were then stained and the remaining cells were counted. Five high-powered fields were counted for each membrane.

In vivo Metastasis

MDA-MB-231 cells that had been engineered to stably express firefly luciferase (MDA-MB-231-Luc-D3H2LN) (Xenogen Corporation) were infected with lentiviruses carrying empty vector, LSD1 expression construct, control siRNA, or LSD1 siRNA. These cells were inoculated into the left abdominal mammary fat pad (2×10^6 cells) or injected into the lateral tail vein (1×10^6 cells) or the left ventricle (1×10^5 cells) of 6-week-old female SCID mice. For bioluminescence imaging, mice were anesthetized and given 150 μg/g of D-luciferin in PBS by i.p. injection. Fifteen minutes after injection, bioluminescence was imaged with a charge-coupled device camera (IVIS; Xenogen). Bioluminescence images were obtained with a 15 cm field of view, binning (resolution) factor of 8, 1/f stop, open filter, and an imaging time of 30 s to 2 min. Bioluminescence from relative optical intensity was defined manually, and data were expressed as photon flux (photons·sec^{-1}·cm^{-2}·steradian^{-1}) and were normalized to background photon flux which was defined from a relative optical intensity drawn over a mouse that was not given an injection of luciferin. The difference in animal numbers (n) in relevant groups was due to the animal loss during the experiments. Animal handling and procedures were approved by the Peking University Health Science Center Institutional Animal Care and Use Committee.

Statistical Analysis

Results are reported as mean ± SD. Comparisons were performed using two-tailed paired t test.

Detailed information about the materials and methods can be found in the Supplemental Data.

SUPPLEMENTAL DATA

Supplemental Data include Supplemental Results, Supplemental References, and an Excel spreadsheet and can be found with this article online at http://www.cell.com/supplemental/S0092-8674(09)00710-7.

ACKNOWLEDGMENTS

We thank Joanne Balmer Green (Penn State University) for editorial assistance. This work was supported by grants (30830032, 30621002 and 30470912, to Y.S.) from the National Natural Science Foundation of China and grants (863 Program: 2006AA02Z466 and 973 Program: 2005CB522404 and 2007CB914503, to Y.S.) from the Ministry of Science and Technology of China.

Received: November 6, 2008
Revised: February 10, 2009
Accepted: May 13, 2009
Published: August 20, 2009

REFERENCES

Bowen, N.J., Fujita, N., Kajita, M., and Wade, P.A. (2004). Mi-2/NuRD: multiple complexes for many purposes. Biochim. Biophys. Acta *1677*, 52–57.

Cheng, X., and Zhang, X. (2007). Structural dynamics of protein lysine methylation and demethylation. Mutat. Res. *618*, 102–115.

Denslow, S.A., and Wade, P.A. (2007). The human Mi-2/NuRD complex and gene regulation. Oncogene *26*, 5433–5438.

Di Stefano, L., Ji, J.Y., Moon, N.S., Herr, A., and Dyson, N. (2007). Mutation of Drosophila Lsd1 disrupts H3–K4 methylation, resulting in tissue-specific defects during development. Curr. Biol. *17*, 808–812.

Dumont, N., and Arteaga, C.L. (2003). Targeting the TGF beta signaling network in human neoplasia. Cancer Cell *3*, 531–536.

Forneris, F., Binda, C., Battaglioli, E., and Mattevi, A. (2008). LSD1: oxidative chemistry for multifaceted functions in chromatin regulation. Trends Biochem. Sci. *33*, 181–189.

Fujita, N., Jaye, D.L., Kajita, M., Geigerman, C., Moreno, C.S., and Wade, P.A. (2003). MTA3, a Mi-2/NuRD complex subunit, regulates an invasive growth pathway in breast cancer. Cell *113*, 207–219.

Huang, J., Sengupta, R., Espejo, A.B., Lee, M.G., Dorsey, J.A., Richter, M., Opravil, S., Shiekhattar, R., Bedford, M.T., Jenuwein, T., et al. (2007). p53 is regulated by the lysine demethylase LSD1. Nature *449*, 105–108.

Kahl, P., Gullotti, L., Heukamp, L.C., Wolf, S., Friedrichs, N., Vorreuther, R., Solleder, G., Bastian, P.J., Ellinger, J., Metzger, E., et al. (2006). Androgen receptor coactivators lysine-specific histone demethylase 1 and four and a half LIM domain protein 2 predict risk of prostate cancer recurrence. Cancer Res. *66*, 11341–11347.

Kumar, R., Wang, R.A., and Bagheri-Yarmand, R. (2003). Emerging roles of MTA family members in human cancers. Semin. Oncol. *30*, 30–37.

Kwon, Y.S., Garcia-Bassets, I., Hutt, K.R., Cheng, C.S., Jin, M., Liu, D., Benner, C., Wang, D., Ye, Z., Bibikova, M., et al. (2007). Sensitive ChIP-DSL technology reveals an extensive estrogen receptor alpha-binding program on human gene promoters. Proc. Natl. Acad. Sci. USA *104*, 4852–4857.

Lan, F., Nottke, A.C., and Shi, Y. (2008). Mechanisms involved in the regulation of histone lysine demethylases. Curr. Opin. Cell Biol. *20*, 316–325.

Laping, N.J., Grygielko, E., Mathur, A., Butter, S., Bomberger, J., Tweed, C., Martin, W., Fornwald, J., Lehr, R., Harling, J., et al. (2002). Inhibition of transforming growth factor (TGF)-beta1-induced extracellular matrix with a novel

inhibitor of the TGF-beta type I receptor kinase activity: SB-431542. Mol. Pharmacol. *62*, 58–64.

Lee, M.G., Wynder, C., Bochar, D.A., Hakimi, M.A., Cooch, N., and Shiekhattar, R. (2006). Functional interplay between histone demethylase and deacetylase enzymes. Mol. Cell. Biol. *26*, 6395–6402.

Lee, M.G., Wynder, C., Cooch, N., and Shiekhattar, R. (2005). An essential role for CoREST in nucleosomal histone 3 lysine 4 demethylation. Nature *437*, 432–435.

Manavathi, B., and Kumar, R. (2007). Metastasis tumor antigens, an emerging family of multifaceted master coregulators. J. Biol. Chem. *282*, 1529–1533.

Massague, J. (2008). TGF[beta] in Cancer. Cell *134*, 215–230.

Massague, J., Blain, S.W., and Lo, R.S. (2000). TGFbeta signaling in growth control, cancer, and heritable disorders. Cell *103*, 295–309.

Mukherjee, S., and Mitra, S. (2005). Hidden Markov Models, grammars, and biology: a tutorial. J. Bioinform. Comput. Biol. *3*, 491–526.

Padua, D., Zhang, X.H., Wang, Q., Nadal, C., Gerald, W.L., Gomis, R.R., and Massague, J. (2008). TGFbeta primes breast tumors for lung metastasis seeding through angiopoietin-like 4. Cell *133*, 66–77.

Sasai, N., Yakura, R., Kamiya, D., Nakazawa, Y., and Sasai, Y. (2008). Ectodermal factor restricts mesoderm differentiation by inhibiting p53. Cell *133*, 878–890.

Shang, Y. (2006). Molecular mechanisms of oestrogen and SERMs in endometrial carcinogenesis. Nat. Rev. Cancer *6*, 360–368.

Shang, Y., and Brown, M. (2002). Molecular determinants for the tissue specificity of SERMs. Science *295*, 2465–2468.

Shang, Y., Hu, X., DiRenzo, J., Lazar, M.A., and Brown, M. (2000). Cofactor dynamics and sufficiency in estrogen receptor-regulated transcription. Cell *103*, 843–852.

Shi, B., Liang, J., Yang, X., Wang, Y., Zhao, Y., Wu, H., Sun, L., Zhang, Y., Chen, Y., Li, R., et al. (2007). Integration of estrogen and Wnt signaling circuits by the polycomb group protein EZH2 in breast cancer cells. Mol. Cell. Biol. *27*, 5105–5119.

Shi, Y. (2007). Histone lysine demethylases: emerging roles in development, physiology and disease. Nat. Rev. Genet. *8*, 829–833.

Shi, Y., Lan, F., Matson, C., Mulligan, P., Whetstine, J.R., Cole, P.A., and Casero, R.A. (2004). Histone demethylation mediated by the nuclear amine oxidase homolog LSD1. Cell *119*, 941–953.

Shi, Y.J., Matson, C., Lan, F., Iwase, S., Baba, T., and Shi, Y. (2005). Regulation of LSD1 histone demethylase activity by its associated factors. Mol. Cell *19*, 857–864.

Siegel, P.M., and Massague, J. (2003). Cytostatic and apoptotic actions of TGF-beta in homeostasis and cancer. Nat. Rev. Cancer *3*, 807–821.

Thiery, J.P. (2002). Epithelial-mesenchymal transitions in tumour progression. Nat. Rev. Cancer *2*, 442–454.

Wang, G.G., Allis, C.D., and Chi, P. (2007a). Chromatin remodeling and cancer, Part I: Covalent histone modifications. Trends Mol. Med. *13*, 363–372.

Wang, J., Scully, K., Zhu, X., Cai, L., Zhang, J., Prefontaine, G.G., Krones, A., Ohgi, K.A., Zhu, P., Garcia-Bassets, I., et al. (2007b). Opposing LSD1 complexes function in developmental gene activation and repression programmes. Nature *446*, 882–887.

Welch, D.R., Fabra, A., and Nakajima, M. (1990). Transforming growth factor beta stimulates mammary adenocarcinoma cell invasion and metastatic potential. Proc. Natl. Acad. Sci. USA *87*, 7678–7682.

Wu, H., Chen, Y., Liang, J., Shi, B., Wu, G., Zhang, Y., Wang, D., Li, R., Yi, X., Zhang, H., et al. (2005). Hypomethylation-linked activation of PAX2 mediates tamoxifen-stimulated endometrial carcinogenesis. Nature *438*, 981–987.

Yamazaki, K., Crowe, D.L., and Shuler, C.F. (2006). Hunchback sequence binding protein suppresses mouse TGF-beta3 promoter in vitro. Biochem. Biophys. Res. Commun. *346*, 802–809.

Yang, J., and Weinberg, R.A. (2008). Epithelial-mesenchymal transition: at the crossroads of development and tumor metastasis. Dev. Cell *14*, 818–829.

Yang, L., Huang, J., Ren, X., Gorska, A.E., Chytil, A., Aakre, M., Carbone, D.P., Matrisian, L.M., Richmond, A., Lin, P.C., et al. (2008). Abrogation of TGF beta signaling in mammary carcinomas recruits Gr-1+CD11b+ myeloid cells that promote metastasis. Cancer Cell *13*, 23–35.

Ye, Z., Yu, X., and Cheng, L. (2008). Lentiviral gene transduction of mouse and human stem cells. Methods Mol. Biol. *430*, 243–253.

Yin, N., Wang, D., Zhang, H., Yi, X., Sun, X., Shi, B., Wu, H., Wu, G., Wang, X., and Shang, Y. (2004). Molecular Mechanisms Involved in the Growth Stimulation of Breast Cancer Cells by Leptin. Cancer Res. *64*, 5870–5875.

You, A., Tong, J.K., Grozinger, C.M., and Schreiber, S.L. (2001). CoREST is an integral component of the CoREST- human histone deacetylase complex. Proc. Natl. Acad. Sci. USA *98*, 1454–1458.

Zavadil, J., and Bottinger, E.P. (2005). TGF-beta and epithelial-to-mesenchymal transitions. Oncogene *24*, 5764–5774.

Zhang, H., Sun, L., Liang, J., Yu, W., Zhang, Y., Wang, Y., Chen, Y., Li, R., Sun, X., and Shang, Y. (2006). The catalytic subunit of the proteasome is engaged in the entire process of estrogen receptor-regulated transcription. EMBO J. *25*, 4223–4233.

Zhang, H., Yi, X., Sun, X., Yin, N., Shi, B., Wu, H., Wang, D., Wu, G., and Shang, Y. (2004). Differential gene regulation by the SRC family of coactivators. Genes Dev. *18*, 1753–1765.

Zhang, Y., Zhang, H., Liang, J., Yu, W., and Shang, Y. (2007). SIP, a novel ankyrin repeat containing protein, sequesters steroid receptor coactivators in the cytoplasm. EMBO J. *26*, 2645–2657.